Int. J. Engng Ed. Vol. 8, No. 3, pp. 228–234, 1992
Printed in Great Britain.

0742–0269/91 $3.00+0.00

PC-aided Electromagnetic Analysis of Permanent Magnet Synchronous Motors*

K. T. CHAU
Department of Electrical Engineering, Hong Kong Polytechnic, Hung Hom, Kowloon, Hong Kong

This paper draws attention to the application of the finite element method as well as the graphical and interactive pre- and post-processing to the electromagnetic analysis of permanent magnet (PM) synchronous motors. As the computing environment is only an ordinary PC, it is a very useful and economical educational tool. The techniques of implementation using C++ and the application of the software for design optimization of PM synchronous motors are described.

INTRODUCTION

THE revolutionary improvements in permanent magnet (PM) materials in recent years and the ingenious use of these materials in machine applications have initiated a succession of important developments. Increasingly, PM synchronous motors have established an important role in high-performance drive systems. High-field synchronous motors, making use of high-energy rare-earth magnets, have found increasing acceptance for a range of applications. These motors have the prospect of high efficiency, leading to a lifetime cost superior to that of standard induction motors [1, 2]. A number of manufacturers are now offering a range of PM motors to compete in the induction motor market.

Owing to the complicated geometry of PM synchronous motors, magnetic properties of PM materials and saturation effects in magnetic materials, the magnetic equivalent circuit approach becomes ill-suited and obsolete. On the contrary, the numerical approach for electromagnetic analysis is becoming attractive. In fact, the increased importance of electromagnetic analysis has stimulated the developments of computational methods and computer facilities [3–5]. As the finite elements method (FEM) is regarded as one of the most powerful and popular tools in electromagnetic analysis [6,7], it is adopted as a tool for the design of PM synchronous motors.

Unfortunately, the computing environments for FEM-based electromagnetic analysis usually involve mainframes, minicomputers or workstations [8, 9]. The powerful computing capabilities and wonderful graphics functions of these computers are undoubtedly essential for industrial applications; however, it seems to be too expensive and bulky for educational purposes. Although recently some software packages have been available for teaching FEM in electromagnetic analysis [10], it is far from applicable to the electromagnetic analysis of electrical machines, especially for PM synchronous motors, which involve complex geometry, PM and magnetic materials, and three-phase stator winding.

In this paper, the FEM-based electromagnetic analysis of PM synchronous motors implementing on an ordinary PC is presented. The software programmed in C++ language incorporates the FEM calculation as well as the pre- and post-processing capabilities. As visualization combats complexity, the pre- and post-processing are enhanced by computer graphics. Hence, the developed software can be manipulated interactively and user-friendly.

PM SYNCHRONOUS MOTORS

Two major classifications of PM synchronous motors are the surface-magnet type where the magnets are mounted on the magnetic outside of the rotor, and the interior-magnet type where the magnets are mounted inside the magnetic structure of the rotor. As the stator of a PM synchronous motor is very similar to that of a polyphase induction motor, the typical rotor geometries of the exterior-magnet type and interior-magnet type are shown in Figs 1(a) and (b) respectively.

Because the reluctance of the PM material is almost the same as that of an equivalent volume of air, the d- and q-axis reactances of the surface-magnet type motor are essentially equal and the value corresponds to a large equivalent air gap. This large equivalent air gap weakens the armature reaction effect and therefore the operation is typically restricted to a constant torque region. Also, because the magnets are surface-mounted on the rotor periphery, it is difficult to maintain mechanical integrity of the rotor at high speed.

When the magnets are extended in the radial direction and located in the interpolar space of the rotor as shown in Fig. 1(b), the d-axis armature

* Paper accepted 20 July 1992.

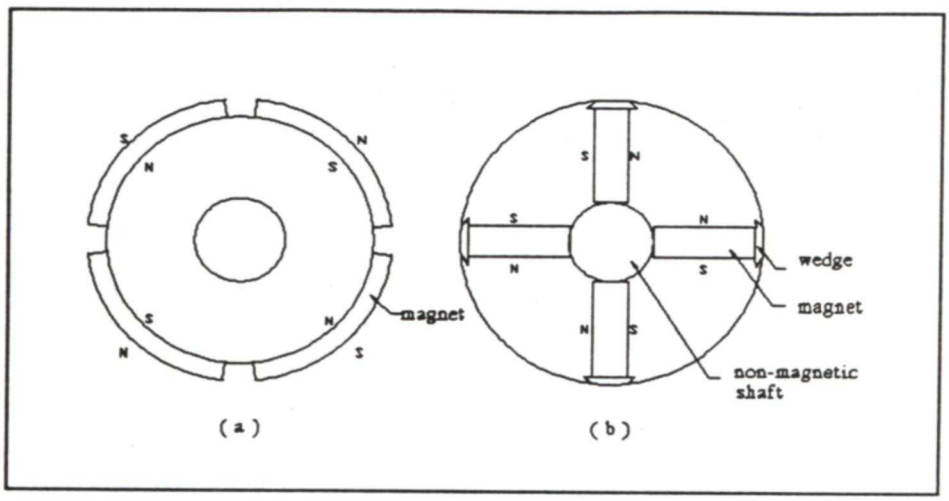

Fig. 1. PM rotor geometries

reactance (X_{ad}) is lower than the q-axis one (X_{aq}) due to the presence of low permeability PM materials in the d-axis armature flux path (on the contrary, X_{ad} is greater than X_{aq} for conventional salient-pole synchronous machines). This location allows the flux per pole to be contributed by two magnets instead of one, leading to air-gap flux concentration. Because the magnets are physically protected, it is capable of withstanding a high-speed operation.

PROGRAMMING LANGUAGE

Instead of the traditionally used programming language such as PASCAL, FORTRAN or ADA, the developed software is programmed by using C++ language. Its appeal is due not only to the popularity of its parent C language, but also to its data abstraction and object-oriented features. C++ has a well-structured programming style, which helps to make the program understandable and maintainable. In addition, it provides a pre-defined data-type so-called 'complex'. This data-type is very useful during the manipulation of complex variables or functions, which are largely involved in the implementation of FEM. As C++ facilitates the use of windows, graphics and mouse, it enhances the implementation of interactive and graphical pre- and post-processing on an ordinary PC. C++ also provides the pointer types, which are used to keep track of dynamically allocated objects for flexibility in data structures.

Similar to its parent C language, C++ is so portable that the developed software can be easily transported to other computing environments such as other PCs, mainframes, minicomputers or workstations.

FINITE ELEMENT METHOD

The finite element solution of magnetic field problems was originally proposed by Silvester and Chari [3]. As the field quantities of an electromagnetic device can be generally derived from potentials, the magnetic field distribution of the interested region is usually described by a partial differential equation of these potentials. The commonly adopted potentials are the vector magnetic potential, the scalar magnetic potential and the vector electric potential. For the electromagnetic analysis of a motor, a 2-D FEM is preferred to a 3-D FEM because the overhang leakage flux of the motor is relatively insignificant while the corresponding computation program and time are much shorter, which are essential during the implementation of FEM on a PC.

By selecting the x–y plane as the cross-section of the motor and the z-axis along its axial direction, the partial differential equation describing the magnetic field distribution in domain Ω is given by

$$\Omega: \frac{\partial}{\partial x}\left(\frac{1}{\mu}\frac{\partial \mathbf{A}}{\partial x}\right)+\frac{\partial}{\partial y}\left(\frac{1}{\mu}\frac{\partial \mathbf{A}}{\partial y}\right)=-\mathbf{J} \qquad (1)$$

where $\mathbf{A}$ = vector magnetic potential, $\mathbf{J}$ = current density and μ = magnetic permeability.

In applying the FEM, the region of interest is divided into small but finite elements. The elements completely cover the region without any overlapping and an individual element does not cross a material boundary. To first order, the potential varies linearly between nodes and the magnetic flux density is then constant within each element. Thus the magnetic permeability of each element is constant. The source current density is also assumed to be constant within each element associated with a winding. To second order, the potential varies quadratically in each direction and this function needs six nodes for each triangular

element. If the triangles are small enough, first-order triangular elements with only three corner nodes are preferred due to its linear property as well as sufficient accuracy.

By setting the first type S_1 and the second type S_2 boundary conditions of the domain Ω

$$S_1: \quad \mathbf{A} = \mathbf{A}_o$$
$$S_2: \quad \frac{\partial \mathbf{A}}{\partial n} = -\mu \mathbf{H}_t \tag{2}$$

where, $\mathbf{A}_o$ = vector magnetic potential in the first type of boundary, and $\mathbf{H}_t$ = tangential magnetic field in the second type of boundary, and using the variational principle, the solution of (1) can be obtained by solving a linearized matrix equation:

$$[K][A] = [R] \tag{3}$$

The K-matrix depends on the discretization of the domain Ω while the R-matrix depends on the current excitation. The A-matrix is a matrix variable which contains the vector magnetic potential of each node. This matrix equation can be solved by the Gauss' elimination or the Newton–Raphson's iteration.

In general, the matrices involved in the computation are stored in arrays. For an educational-purpose problem of 200 nodes, however, the K-matrix consists of 200×200 floating-point elements, requiring 160 kB of RAM to store this single matrix. As there are some temporary counterparts of the K-matrix during the computation, it is very difficult to make use of arrays to implement the FEM on an ordinary PC, where the maximum usable RAM is limited to 640 kB under DOS operating system. Moreover, most of the compilers cannot allow the user to define an array greater than 64 kB of RAM due to the segmentation architecture employed in ordinary PCs. Fortunately, the K-matrix has the property of sparsity such that most of its elements are zero. By storing only the non-zero term K_{ij} in the i-th row and j-th column of the K-matrix, the corresponding sparse matrix $[K_s]$ is created, and each of its elements is in form of

$$[i\ j\ K_{ij}] \tag{4}$$

In addition, the non-zero elements of the K-matrix are clustered in a narrow band along the matrix diagonal. Since the width of the band is characterized by the numbering of the nodes, it can be reduced by numbering the nodes across the shortest dimension of the domain Ω. Thus a proper numbering of the nodes can further reduce the required memory to store the K_s-matrix. Besides the sparsity, the K-matrix possesses the property of symmetry so that only the upper-half triangle (including the matrix diagonal) is transformed to the K_s-matrix. Ultimately, it is observed that the size of the K_s-matrix is only about 20% of the original K-matrix. Furthermore, instead of using an array to store the K_s-matrix, the pointer variable in C++ language is employed to implement the K_s-matrix so as to override the 64 kB barrier of an array.

DESIGN OF PM SYNCHRONOUS MOTORS

For a four-pole PM synchronous motor, the interested domain is only one-quarter of the whole cross-section. The boundary conditions of the domain are

$$\mathbf{A}|_L = 0 \tag{5}$$

on the outer surfaces of the stator and the shaft as well as the anti-symmetry periodicity

$$\mathbf{A}|_{L_1} = -\mathbf{A}|_{L_2} \tag{6}$$

on the boundaries connecting the shaft with the outer surface of the stator. Since the demagnetization curve of rare-earth PM materials (e.g. neodymium-iron-boron and samarium-cobalt) is almost linear, the effect of the PM within the domain is considered as a surface current density of $\mathbf{H}_c$, which provides an interface condition

$$\left.\frac{\partial \mathbf{A}}{\partial n}\right|_{L^+} - \left.\frac{\partial \mathbf{A}}{\partial n}\right|_{L^-} = \mu \mathbf{H}_c \tag{7}$$

Owing to the saturation effect of the magnetic material, its B-H characteristic is modelled by a spline cubic curve or a table look-up. Although the table look-up method incorporating the interpolation technique can provide a faster computation, the spline cubic curve is adopted because it does not require a lot of memory space to store the table.

By initializing the magnetic permeability of each element within the domain, the vector magnetic potential of each node can be determined from the matrix equation shown in (3). The magnetic permeability of each element corresponding to its magnetic flux density obtained from the previous solution is successively modified. The convergence criterion is satisfied when the changes in magnetic permeability over each element is smaller than the tolerance. The flowchart of this iterative process is shown in Fig. 2.

By using the FEM to determine the no-load e.m.f. (E_o), d-axis armature reactance (X_{ad}) and q-axis armature reactance (X_{aq}), other motor parameters including the output torque, efficiency, power factor and load angle can then be deduced. When the external source current density is set to zero, the magnetic field distribution is excited by the magnets only, hence the induced e.m.f. is E_o. When the surface current density is set to zero, the magnetic field distribution is excited by the stator armature current only, hence the induced e.m.f. is the armature reaction voltage (E_a). By rotating the rotor such that its d-axis is aligned with the centre of phase A, the resultant armature field induces the d-axis armature reaction voltage (E_{ad}) and X_{ad} can be calculated as follows

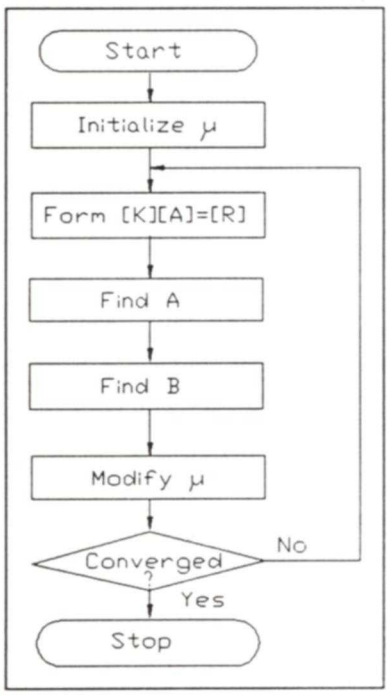

Fig. 2. Flowchart of iteration

$$X_{ad} = \frac{E_{ad}}{I_A} \tag{8}$$

where I_A is the current of phase A. Similarly, by adjusting the q-axis of the rotor in alignment with the centre of phase A, the resultant armature field induces the q-axis armature reaction voltage (E_{aq}) and X_{aq} can be determined as follows

$$X_{aq} = \frac{E_{aq}}{I_A} \tag{9}$$

GRAPHICS ENHANCED PRE- AND POST-PROCESSING

In order to illustrate the pre- and post-processing of the FEM-based electromagnetic analysis, a typical interior-type PM synchronous motor shown in Fig. 1(b) is selected as an example. First, the pre-processing can be accomplished by an interactive mesh generator, which translates the interested domain of the motor geometry into nodes and triangles. Having inputted the physical dimensions of the motor, the nodes are automatically generated. The types of boundary are selected interactively by using the on-line cursor as shown in Fig. 3. After generating the triangular mesh, each of the elements is then identified interactively, such that it belongs to the stator iron core, stator slot, air gap, rotor iron core, magnet or non-magnetic wedge, which is shown in Fig. 4.

The database resulting from the FEM-based electromagnetic analysis consists of the vector magnetic potentials, magnetic flux densities and magnetic permeabilities. The analysis of these massive amounts of information can hardly be performed accurately and efficiently without making use of computer graphics for post-processing. Generally, there are two approaches to represent such massive databases. The contour-based representation of magnetic flux density distribution has been widely used as shown in Fig. 5. Since the equipotential contour of the vector magnetic potential represents the magnetic flux line, the more the contours lie within a region the higher is the magnetic flux density. Alternatively, with the employment of graphics functions provided by C++, the magnetic flux density can be directly represented by shaded coloured elements as shown in Fig. 6. Besides using shaded colours to depict the magnetic flux density distribution, the actual value of the magnetic flux

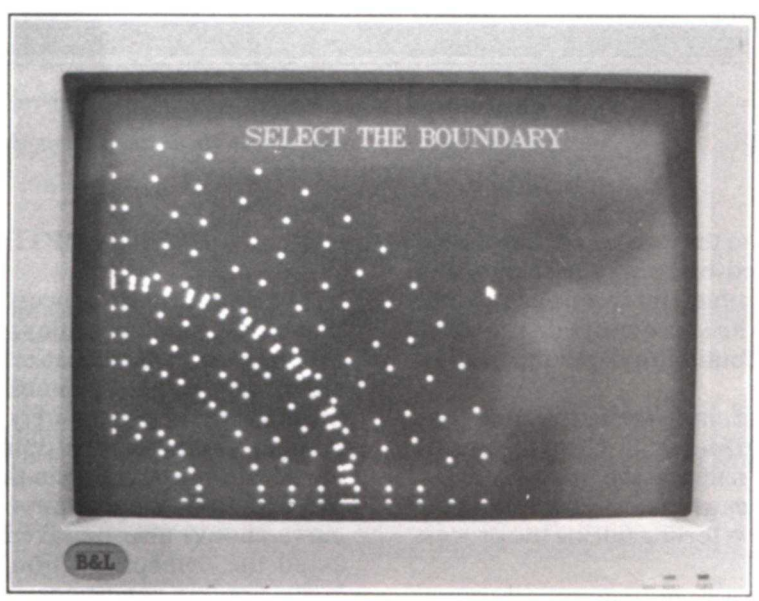

Fig. 3. Selection of boundary

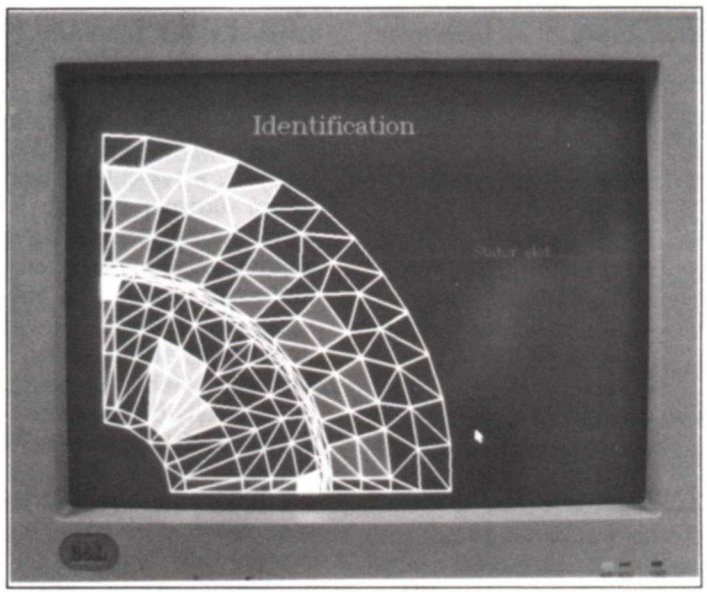

Fig. 4. Identification of element

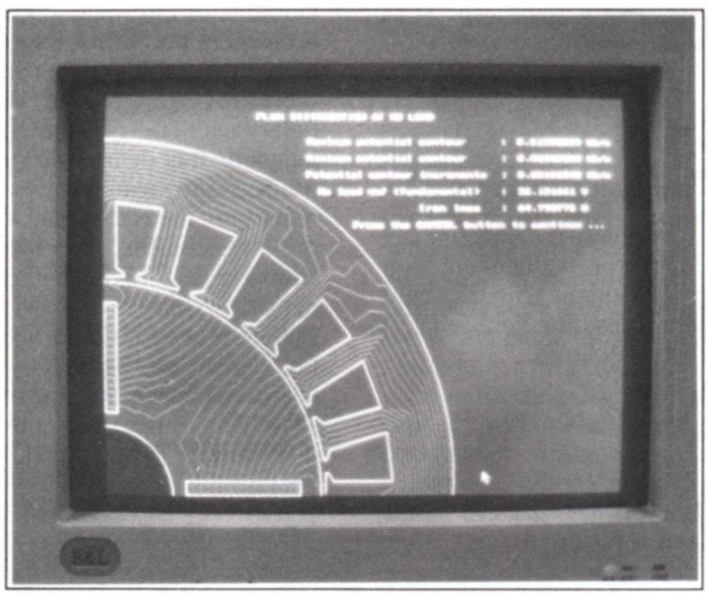

Fig. 5. Contour-based magnetic field distribution

density corresponding to the location of the on-line cursor can be displayed by using the facilities of windows and mouse. In fact, this approach can be extended to represent the loss density distribution, the thermal field distribution and the mechanical stress distribution.

Therefore, the visual and interactive pre- and post-processing of FEM-based electromagnetic analysis can greatly facilitate the motor design. Moreover, the computer graphics can provide the designer with an intuitive feeling during the process of design optimization.

DESIGN OPTIMIZATION

The optimization process includes the minimization of PM material outlay as well as the maximization of iron core utilization. By iteratively varying the magnet height, thickness and axial length while keeping E_o approximately constant, the magnet material outlay can be optimized without causing unnecessary saturation in the iron core. Moreover, the PM operating point on its demagnetization curve should also be taken into account so as to avoid the demagnetization during the starting or heavy loading conditions. The flowchart of design optimization is shown in Fig. 7.

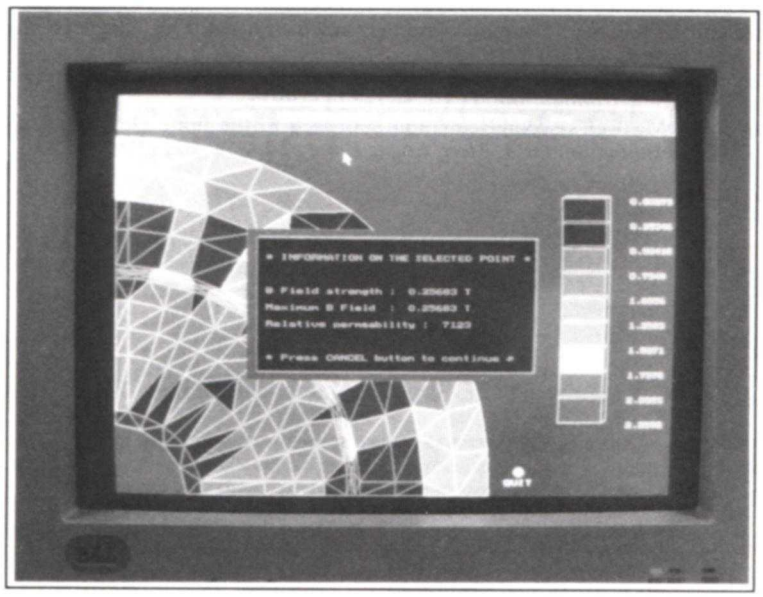

Fig. 6. Colour-based magnetic field distribution

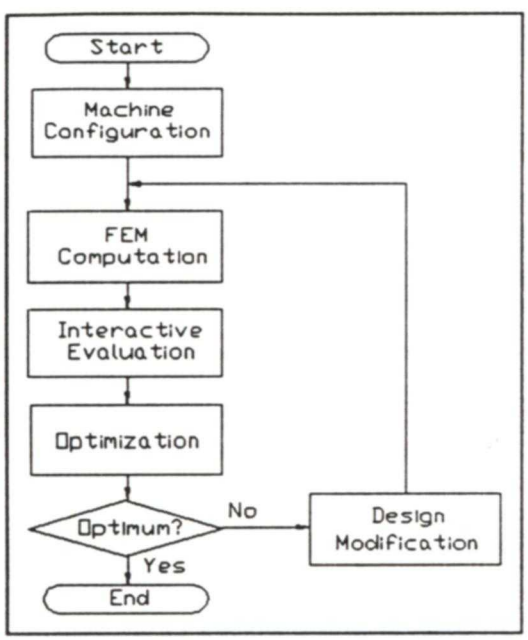

Fig. 7. Flowchart of optimization

CONCLUSIONS

As it is ill-suited to apply the traditional magnetic equivalent circuit approach to the analysis of PM synchronous motors, a FEM-based electromagnetic field approach is proposed and implemented on an ordinary PC, which is more economical and less bulky for the laboratories in polytechnics and universities. The software is fully developed by using C++ language, which facilitates the complex variable calculation as well as the graphical and interactive pre- and post-processing for the FEM-based electromagnetic analysis. The design optimization has been focused on the minimization of PM material outlay, the maximization of iron core utilization and selection of PM operating point.

Acknowledgements—The author thanks Mr C. S. Wong for his tireless efforts during the software development stage.

REFERENCES

1. K. J. Binns and T. M. Wong, Analysis and performance of a high-field permanent-magnetic synchronous machine. *IEEE Proc. B*, **131**, 252–257 (1984).
2. M. A. Rahman and G. R. Slemon, Promising application of neodymium boron iron magnets in electrical machines. *IEEE Trans. Magn.*, **21**, 1712–1716 (1985).
3. P. Sylvester and M. V. K. Chari, Finite element solution of saturable magnetic field problems. *IEEE Trans. Power Appar. Syst.*, **89**, 1642–1651 (1970).
4. P. Hammond and D. Baldomir, Dual energy methods in electromagnetism using tubes and slices. *IEEE Proc. A*, **135**, 167–172 (1988).
5. S. A. Nasar and G. Xiong, Determination of the field of a permanent magnet disk machine using the concept of magnetic charge. *IEEE Trans. Magn.*, **24**, 2038–2044 (1988).
6. A. B. J. Reece, Electrical machines and electromagnetics—computer aids to design, *GEC Rev.*, **5**, 34–41 (1989).
7. S. J. Salon, Finite-element analysis of electric machinery. *IEEE Comput. Appl. Power Mag.*, April, 29–32 (1990).

8. C. C. Chan and K. T. Chau, Computer graphics aided design for an advanced electrical motor. *Comput. Aid. Engng J.*, **7**, 72–74 (1990).
9. C. C. Chan and K. T. Chau, Design of electrical machines by the finite element method using distributed computing. *Comput. Ind. J.*, **17**, 367–374 (1991).
10. J. R. Cardoso, A Maxwell's second equation approach to the finite element method applied to magnetic field determination. *Int. J. Elect. Engng Educ.*, **24**, 259–272 (1987).